Materials Science & Engineering A 639 (2015) 732–738

Contents lists available at ScienceDirect

Materials Science & Engineering A

journal homepage: www.elsevier.com/locate/msea

Effect of carbon content on the microstructure and creep properties of a 3rd generation single crystal nickel-base superalloy

X.W. Li [a], T. Liu [a], L. Wang [a,b,*], X.G. Liu [a], L.H. Lou [a], J. Zhang [a,b]

[a] Superalloys Division, Institute of Metal Research, Chinese Academy of Sciences, Shenyang 110016, China
[b] Shenyang National Laboratory for Materials Science, Institute of Metal Research, Chinese Academy of Sciences, Shenyang 110016, China

ARTICLE INFO

Article history:
Received 14 November 2014
Received in revised form
12 May 2015
Accepted 13 May 2015
Available online 27 May 2015

Keywords:
Carbides
Microporosity
X-ray computed tomography
Creep property
Nickel-base superalloys

ABSTRACT

Effect of carbon content on the microstructure and creep properties of a 3rd generation single crystal nickel-base superalloy has been investigated by the scanning electron microscope, X-ray computed tomography and electron probe microanalyzer. With the increase of the carbon content, MC carbides evolve from octahedral to well-developed dendrite, which promotes the formation of microporosity. Moreover, the volume fraction of porosity increases in the experimental alloys after solution heat treatment. As a result, the increase in the size of MC carbides and the porosity has a detrimental effect on the low temperature and high stress creep behavior of the alloys. The specimen crept at 850 °C and 586 MPa with the carbon content of 430 ppm shows the shortest rupture life due to the largest primary creep strain. However, the creep behavior of the alloy at 1120 °C and 140 MPa gets better as the carbon content increases from 88 to 430 ppm. TCP phase is observed near the fracture surfaces of the alloys, which explores as a potential cause for the creep rupture. However, the formation of TCP phase is effectively suppressed for decreasing segregation of the alloying elements, which results in the improvement of the creep life in the alloy with 430 ppm carbon at 1120 °C and 140 MPa.

1. Introduction

Single crystal (SX) superalloys have been widely used in advanced turbine engines for hot components. To further enhance their high temperature capability, the level of refractory elements such as tungsten and rhenium in the advanced SX superalloys has been gradually increased. However, there is a great tendency for the formation of grain defects (strays, low angle grain boundaries, freckles, etc.) in these alloys [1–3]. Therefore, trace elements such as carbon and boron are reintroduced into SX superalloys for grain boundary reinforcement [4,5] and reducing casting defects during solidification [6–8].

The formation of grain defects in the SX superalloys with the addition of carbon can be effectively suppressed [6,7]. However, conflicting results involving the role of carbon on the creep property of SX alloy have been reported. It has been found that the creep life in the carbon modified SX alloy at 850 °C/430 MPa is improved, but the creep life at 1050 °C/165 MPa decreases [9]. Contrary results were observed by Liu et.al [10]. Kong and Wasson also reported that carbon has a detrimental effect on creep life under different conditions [11,12]. It is necessary to clarify the influence of carbon on the creep life in SX superalloys.

Creep rupture is associated with a number of microstructural features, including MC carbides, porosity and TCP formation. It has been confirmed that morphology of MC carbides transforms from blocky to script-like and the volume fraction of γ/γ' eutectic is reduced by carbon additions [13–15]. However, there are controversial opinions concerning the role of carbon during the formation of porosity. Liu and Chen [8,16] found that the formation of porosity is suppressed by the addition of carbon due to volume expansion of MC carbides. However, an increase volume fraction of porosity is observed by Al-Jarba and Culter [7,17] with carbon additions. Moreover, the H-pore formed during homogenization has been observed, and the volume fraction of H-pore exhibits the same level as that of S-pore formed during solidification [18–20]. The two kinds of pores have not been distinguished. In this study, the three dimensional information of S-pore and H-pore has been investigated by X-ray computed tomography (XCT).

The topologically close packed (TCP) phase is prone to form during the rafting creep [21,22]. The brittle and needle-like phase depletes strengthening elements from the matrix and is susceptible to crack during creep deformation. Retardation of TCP formation in carbon modified alloy RR2072 has been observed [23], while Qin and Kong [24,25] reported that TCP phase initiates in the vicinity of MC carbides.

Therefore, the aim of the present study is to illustrate the effect

* Corresponding author. Tel.: +86 24 23971276; fax: +86 24 23971712.
E-mail address: wangli@imr.ac.cn (L. Wang).

http://dx.doi.org/10.1016/j.msea.2015.05.039
0921-5093/

Table 1
The actual carbon contents of alloys in the present experiment.

	SX-1	SX-2	SX-3
C (ppm)	88	220	430

of carbon on the microstructure involving the porosity, the TCP phase and the creep properties in the SX alloys.

2. Experimental procedure

A 3rd generation nickel-base single crystal (SX) superalloy DD33 with 4% Re (mass fraction, %) was used in the present experiment. The master alloys with three different amounts of carbon were directionally solidified (DS) into $\phi 16 \times 200$ mm SX bars by the high rate solidification (HRS) process. The actual carbon contents of alloys were given in Table 1.

Longitudinal orientation of all SX bars was within 10° deviating from [001] orientation. The samples for comparison of as-cast microstructures (γ/γ' eutectic, porosity and MC carbides) were sectioned perpendicularly to the DS direction and taken from the same location on each SX bar in order to minimize the effect of solidification conditions. To investigate 3-D features of solidification pores (S-pore) and homogenization pores (H-pore) by XCT, the as-cast and solution heat treated samples were machined into cubes of $1 \times 1 \times 1$ mm^3.

Partitioning coefficient of alloying elements in alloys with different carbon contents was measured by electron probe microanalyzer (EPMA). Point scans in dendrite cores and interdendritic regions were performed. The partitioning coefficient, k_i, of each element was identified by dividing the weight percent of each element at the dendrite cores by that in the interdendritic regions. Ten points from each area were averaged to reduce variation.

Following the same heat treatment (1335 °C/10 h, AC+1150 °C/4 h, AC+870 °C/24 h, AC), the first group of samples were exposed at 1100 °C for 1000 h to examine the formation of TCP phase. The second group of heat treated samples were machined into creep specimens with gauge diameter of 5 mm and gauge length of 25 mm along the [001] orientation. Creep tests were carried out at 870 °C/586 MPa and 1120 °C/140 MPa, using FC-20 high temperature creep-testing machines. The microstructure of crept specimens was examined using scanning electron microscope (SEM).

3. Results

3.1. As-cast microstructure

Varying the carbon contents from 88 to 430 ppm, the alloys have similar dendrite arm spacing, but the morphology of MC carbides changes from blocky (Fig. 1a) to script-like (Fig. 1b). These results agree well with previous studies [13–15,26]. Further SEM observations on the deep-etched sample show that the script-like MC carbides actually adopt a dendritic structure (Fig. 1c). These dendritic carbides are rich in Ta and Ti, and have a small amount of Mo, Co and Cr (Table 2).

Table 2
Chemical composition of MC carbides (wt%).

Phase	C	Ti	Cr	Co	Ni	Mo	Ta
MC	13	2	2	2	7	3	71

Table 3
Volume fractions of porosity in as-cast alloys measured by XCT and OM.

C (ppm)	88	220	430
XCT	0.07 ± 0.002	0.08 ± 0.004	0.12 ± 0.006
OM	0.03 ± 0.01	0.05 ± 0.03	0.09 ± 0.05

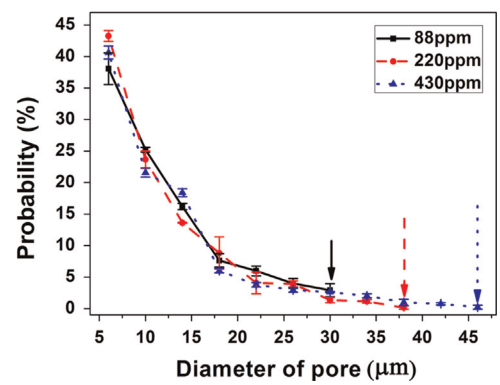

Fig. 2. Distribution of porosity diameter in as-cast alloys with different carbon contents.

The volume fraction of porosity measured by XCT and OM is given in Table 3. The volume fraction of S-pore measured by XCT is 0.07%, 0.08% and 0.12% in the alloys of SX-1, SX-2 and SX-3, respectively. The XCT results are higher, compared with the porosity metallographically measured by OM. The porosity measured by the two different methods are in agreement within the accuracy. Increasing volume fractions of porosity is observed in high carbon modified alloys. Distribution of porosity diameter is illustrated in Fig. 2. The maximum diameter of porosity increases from 30 to 46 μm, with the carbon content increasing from 88 to 430 ppm.

Fig. 3 shows SEM and XCT images of the porosity in the alloy SX-1. SEM observation indicates that porosities are located in the interdendritic regions (Fig. 3a). XCT observation shows that there

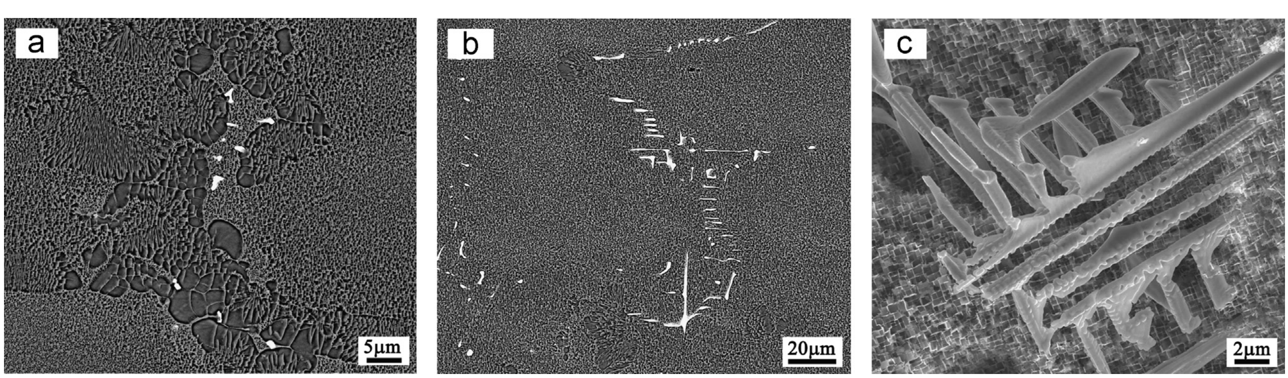

Fig. 1. Morphology of MC carbides in the alloy with different carbon contents: (a) 88 ppm, (b) and (c) 430 ppm.